RSC Advances

ROYAL SOCIETY OF CHEMISTRY

www.rsc.org/advances

Selective Fluorescence Assay of Aluminum and Cyanide Ions Using Chemosensor Containing Naphthol

Soojin Kim,[1§] Jin Young Noh,[2§] Sol Ji Park,[1] Yu Jeong Na,[2] In Hong Hwang,[2] Jisook Min,[3]

Cheal Kim,[2]* Jinheung Kim[1]*

[1]*Department of Chemistry and Nano Science,* Global Top 5 Research Program,

Ewha Womans University, Seoul 120-750, Korea

[2]*Department of Fine Chemistry,*

Seoul National University of Science and Technology, Seoul, Korea

[3]*National Forensic Service, Seoul, 158-707, Korea*

Mailing Address: *Department of Chemistry and Nano Science,*

Ewha Womans University, Seoul 120-750, Korea.

Phone: +82-2-3277-4453

Fax: +82-2-3277-3419

E-mail: chealkim@snust.ac.kr (C. Kim); jinheung@ewha.ac.kr (J. Kim)

[§]Both authors contributed equally to this work

Abstract.

The selective assay of aluminum and cyanide ions is reported using fluorescence enhancement and quenching of a phenol-naphthol based chemosensor (PNI) in aqueous and nonaqueous solvents, respectively. PNI gave no significant fluorescence in water. The binding properties of PNI with metal ions were investigated by UV-vis, fluorescence, and electrospray ionization mass spectrometry in a bis-Tris buffer solution. The addition of aluminum ions switches on the fluorescence of the sensor PNI in water, comparable to relatively very low fluorescence changes in the presence of other various metal ions. The complex stability constant (K_a) for the stoichiometric 1:1 complexation of PNI with aluminium ions was obtained by fluorimetric titrations and NMR experiments. However, upon treatment with cyanide ions, the fluorescence of PNI was selectively turned off and the yellow solution of PNI turned to red in methanol. Other comparable anions, such as F^-, Cl^-, Br^-, I^-, CH_3COO^-, and $H_2PO_4^-$, afforded no apparent fluorescence quenching. The interaction of PNI with cyanide ions were studied by NMR experiments.

Keyword: aluminum ions; fluorescence chemosensor; cyanide ions; naphthol; cell imaging

Introduction.

Fluorescent probes for selective detection of various biologically and environmentally relevant small anions and metal cations have attracted an increasing interest in the lasting impact of their toxic effects in biological systems. Due to the widespread use of aluminum in food and cooking related goods, a possibility of human exposure to aluminum has increased. Long-term intake of excess aluminum ions is possible to spread throughout all tissues in humans and animals, and eventually accumulates in the bone. The iron binding proteins in the human body are the major carrier of Al^{3+} in plasma. Aluminum ions can enter the brain and reach the placenta and fetus by such *in vivo* carriers. Aluminum ions can stay quite a while in various organs and tissues before they are excreted through the urine. In addition, aluminum ions may be one of possible factors of Alzheimer's disease reported to result from the accumulation of oxidative damage induced by metal ions and may result in bad influence to the central nervous system in humans.[1-4] The average daily human intake of aluminum ions recommended by WHO is about 3 ~ 10 mg.[5, 6] In the study of chemosensors for aluminum ion, Schiff base complexes showed various applications, such as analytical, biological, and clinical fields. Recently, Schiff base-type chemosensors have also been reported as a major class for sensing aluminum ions.[7-12]

Cyanide ions are extremely toxic to mammals and lead to death above a certain level. WHO recommends the cyanide concentration in drinking water to be kept lower than ca. 2 μM.[13] Chemicals containing cyanide ions are widely used in electroplating, gold mining, and polymer production.[14-16] Recently, some chemosensors specific for cyanide have been reported based on fatal toxicity of cyanide in biological systems and environment. [17-30] More examples of selective chemosensors for cyanide are needed to develop fast and accurate detection of cyanide in various situations.

In this study, we report the anion and metal cation-binding properties of a new imine probe bearing phenol and naphthol moieties which is the π-conjugated Schiff base receptor. This imine probe exhibited fluorescence enhancement with high selectivity upon binding to aluminum ions in aqueous solution, and fluorescence quenching with high selectivity to cyanide anions in methanol. The *in vivo* application of the probe as an intracellular sensor of Al^{3+} is also reported by confocal fluorescence microscopy.

Results and Discussion.

Fluorometric assay of aluminum ion

The chemosensor, *ortho*-phenol-*ortho*-naphtholmethylimine (PNI) was prepared by the reaction of 1-hydroxy-2-naphthaldehyde and 2-aminophenol with 61 % yield (Scheme 1 and Experimental Section). The binding properties of the PNI receptor was examined towards various metal ions, such as Ag^{+}, Na^{+}, K^{+}, Ca^{2+}, Mg^{2+}, Ni^{2+}, Cd^{2+}, Mn^{2+}, Co^{2+}, Cu^{2+}, Zn^{2+}, Hg^{2+}, Pb^{2+}, Al^{3+}, Sc^{3+}, Cr^{3+}, Fe^{3+}, Ga^{3+}, and In^{3+} (34 equiv each) in 50 mM bis-Tris buffer (pH = 7.0). The fluorescence spectral response in the presence of each metal ion was shown in Figure 1. Relative to no fluorescence of PNI in aqueous solution, significant spectral changes were observed in the case of Al^{3+}. No significant changes observed with other metal ions demonstrate the high selectivity of PNI to other metal ions. PNI is even highly selective for Al^{3+} over Ga^{3+} and In^{3+}.

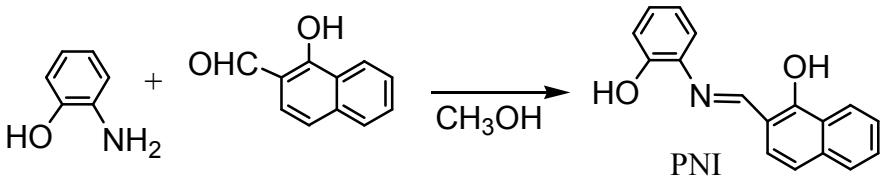

Scheme 1. Synthesis of the fluorescent sensor *ortho*-phenyl-*ortho*-naphtholmethylimine

(PNI)

The turn-on fluorescence response of PNI was observed for Al^{3+} with emission bands at 490 and 515 nm. Upon addition of 34 equiv Al^{3+}, the fluorescence intensity of PNI increased by 100-fold. The fluorescence spectra of PNI progressively changed upon addition of an incremental amount of Al^{3+} (Figure 2a). The fluorometric titration curve showed a steady and smooth increase with increasing Al^{3+} concentration, which demonstrated an efficient fluorescence response (Figure 2b). The binding affinity of PNI towards Al^{3+} was quantified based on fluorescence titration experiments, affording the association constant (K_a) of 2.5 x 10^3 M^{-1} (Supporting Information, Figure S1). Upon binding of Al^{3+}, the aromatic rings of PNI no more rotate around the imine group, and two aromatic rings could be on the same plane to make a good conjugated system through the imine. This conjugation probably caused the fluorescence enhancement. In the case of other metal ions which can bind to PNI in a similar manner, the fluorescence would be quenched by each metal coordination.

The absorption spectra of PNI also changed upon addition of Al^{3+} ions (Figure 3). The bands at 285, 455, and 473 nm decreased and no characteristic new bands appeared.

Figure 4 illustrate the fluorescence response of PNI to Al^{3+} in the presence of other competing metal ions, respectively. Except for Cu^{2+}, Cr^{3+}, and Fe^{3+}, backgrounds of most metal ions do not interfere with the detection of Al^{3+} by PNI in Tris buffer (pH = 7.0). Chemosensors reporting fluorescence studies with Al^{3+} in the presence of competing metal ions showed inhibition by Ag^{+}, Cu^{2+}, Cr^{3+}, and Fe^{3+} [11, 12], but PNI was not significantly inhibited by the other metal ions. In order to understand the interference by Cu^{2+}, Cr^{3+}, and Fe^{3+}, absorption spectra were obtained using the mixtures of Al^{3+} and other metal ions. In the presence of Cu^{2+}, Cr^{3+}, or Fe^{3+}, the absorption spectrum of PNI and Al^{3+} were different from that obtained without

such interfering metal ions. Based on the spectral changes, the inference derived from the displacement of Al^{3+}.

A Job's plot as well as binding analysis using the Benesi-Hildebrand plot established that a 1:1 complex of PNI (Scheme 2 and Figure S2). Al^{3+} could be detected down to 0.13 μM based on the 3α/slope when 5 μM PNI was employed. The 1:1 complex was supported by the electrospray mass spectrum of PNI and Al^{3+} (Figure S3, Supporting Information). The ESI-MS peak at *m/z* = 412.07 (calculated = 412.04) was attributed to $\{[PNI + Al^{3+} + 2NO_3^-]\}^+$.

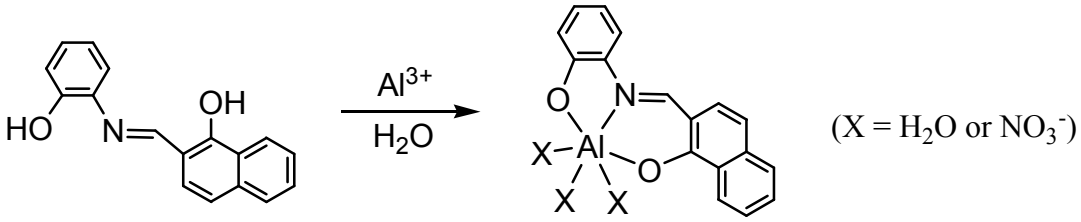

Scheme 2. Proposed structure of a 1:1 complex of PNI and Al^{3+}.

Colorimetric and fluorometric assay of cyanide ion

The anion binding affinity of PNI was evaluated by monitoring their UV-vis and steady-state emission properties as a function of anion concentration in methanol. The changes in the UV-vis spectrum of PNI were observed as a function of CN^- concentration (Figure 5a). The bands at 286, 320, 457, and 480 nm decreased and a new band at 300 nm appeared. Two clear isosbestic points observed at 368 and 400 nm indicated a clean conversion throughout the titration. A photograph of the color changes induced upon anion treatment to methanol solutions of PNI is shown in Figure 5b. An obvious color change from yellow to red was observed only upon treatment with cyanide. Previously, some organic dyes have been reported as colorimetric sensors for cyanide ions, in which all probes were covalently bound with cyanide upon

addition.[22, 23, 29]

The fluorescence spectrum of free PNI showed an emission band at 518 nm. As shown in Figure 6, only cyanide ions caused significant fluorescence changes of PNI compared to other anions examined. The fluorescence maximum was shifted to 540 nm upon treatment with cyanide. The fluorescence responses of PNI were unperturbed by F^-, Cl^-, Br^-, I^-, CH_3COO^-, and $H_2PO_4^-$ at 100-fold excess. The titration experiment showed a progressive intensity decrease at 518 nm (Figure 7).

Further insights into the nature of PNI and cyanide interactions were studied by ^{1}H-NMR titration experiments. Addition of cyanide to PNI did not show any significant changes in the NMR spectra (Figure S4). The well resolved resonance signals of aromatic protons of PNI became a little broad and shifted upon addition of cyanide. Interestingly, the imine proton signal also appeared no evident shift in the absence and presence of cyanide. Usually, the neighboring protons to cyanide bonding covalently to probes were shifted significantly in NMR spectra.[18, 21, 31] Therefore, the fluorescence behavior of PNI towards cyanide can be explained as a deprotonation process of phenol and naphthol (Scheme 3). Such a fluorescence quenching of a probe upon treatment of cyanide was also proposed due to deprotonation.[25]

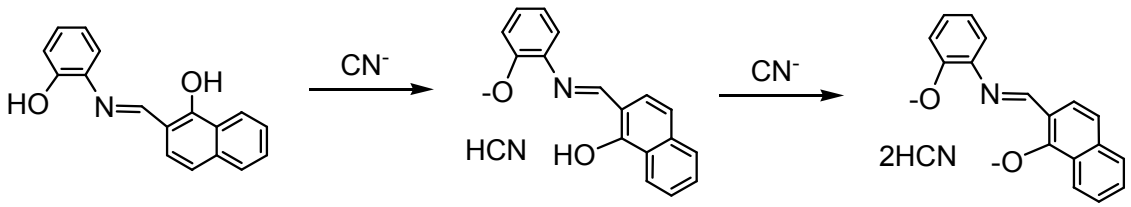

Scheme 3. Proposed structures showing the deprotonation reactions between PNI and CN^-.

Live cell imaging

We examined the bioimaging application of PNI for mapping aluminum ions in living cells. HeLa cells were first exposed to 0 and 1 μM $Al(NO_3)_3$ for 4 h and then incubated with the chemosensor (10 μM) for 20 min. Low background fluorescence was observed in the cells (Figure 8a) that had not been exposed to $Al(NO_3)_3$. The background fluorescence derived from cellular metal ions, such as Na^+, Ca^{2+}, Mg^{2+}, Zn^{2+}, etc, which also afforded low fluorescence with PNI (Figure 8b). Weak but still discernible fluorescence was observed in the cells previously exposed $Al(NO_3)_3$ at 1 μM, compared to the unexposed cells. These results indicate that the fluorescence intensities in the exposed cells depended on the $Al(NO_3)_3$ concentrations. The PNI probe afforded strong fluorescence in the presence of intracellular Al^{3+}, thus demonstrating its suitability for determining the exposure level of cells to aluminum ions.

Conclusions.

We have described a new fluorescent Schiff-base chemosensor PNI for sensing aluminum and cyanide ions. PNI exhibited high selectivity for Al^{3+} in aqueous solution over competing relevant metal ions and a large turn-on response for detecting aluminum ions. In addition, the treatment with anions to the methanol solution leads to different photophysical behaviors. PNI showed the responses specific for cyanide ions, resulting in readily distinguished by color. Furthermore, PNI is capable of mapping aluminum levels in live cells, which might be exploited as specific and effective sensors for intracellular aluminum ions.

Experimental Section.

Materials and Instrumentation

All the solvents and reagents (analytical grade and spectroscopic grade) were obtained from Sigma-Aldrich and used as received. Water was purified with a MilliQ purification system. The metal ion solutions were prepared with metal nitrate salts in methanol. ^{1}H and ^{13}C-NMR spectra were recorded on a Varian 400 spectrometer (Palo Alto, CA, USA). Chemical shifts (δ) are reported in ppm, relative to tetramethylsilane $Si(CH_3)_4$. Absorption spectra were recorded at 25°C using a Perkin-Elmer model Lambda 2S UV/Vis spectrometer (Waltham, MA, USA). Emission spectra were recorded on a Perkin-Elmer LS45 fluorescence spectrometer. Electrospray ionization mass spectra (ESI-MS) were collected on a Thermo Finnigan (San Jose, CA, USA) LCQTM Advantage MAX quadrupole ion trap instrument, by infusing samples directly into the source at 25 μL/min with a syringe pump. The spray voltage was set at 4.7 kV and the capillary temperature at 70 °C. Elemental analysis for carbon, nitrogen, and hydrogen was carried out by using a Flash EA 1112 elemental analyzer (thermo) in Organic Chemistry Research Center of Sogang University, Korea. To confirm the accuracy and reliability of the analytical procedure, the concentrations of various metal ions were checked by inductively coupled plasma (ICP) spectroscopic analysis.

Synthesis of *ortho*-phenyljulolidineimine (PNI)

A solution of 2-aminophenol (0.12 g, 1.1 mmol) in methanol was added to a solution containing 1-hydroxy-2-naphthaldehyde (0.18 g, 1 mmol) in methanol. The reaction mixture was stirred for 5 h at room temperature until an orange precipitate appeared. The resulting precipitate was filtered and washed 2 times with ice methanol. The yield: 0.13 g (61%). ^{1}H NMR (DMSO-d_6, 400 MHz): 14.61 (*d*, *J* = 12 Hz, 1H), 10. 42 (*s*,1H), 8.86 (*d*, *J* = 12 Hz, 1H), 8.32 (*d*, *J* = 8 Hz, 1H), 7.70 (*d*, *J* = 8 Hz, 1H), 7.65 (*m*, 2H), 7.42 (*t*, *J* = 8 Hz, 1H), 7.21 (*d*, *J* = 8 Hz, 1H), 7.09 (*t*, *J* = 8 Hz, 1H), 7.03 (*d*, *J* = 8 Hz, 1H), 6.94 (t, *J* = 8 Hz, 1H), 6.81 (*d*, *J* = 8 Hz, 1H). ^{13}C NMR

(DMSO-d_6, 400 MHz): *d* 171.08, 163.64, 146.84, 136.69, 129.98, 128.54, 128.38, 128.27, 128.00, 127.81, 127.49, 125.25, 124.42, 123.63, 121.67, 120.44, 118.92, 115.61,110.57 ppm. Anal. Calcd for $C_{17}H_{13}NO_2$ (263.09): C, 77.55; H, 4.98; N, 5.32. Found: C, 77.51; H, 5.01; N, 5.28%.

UV-vis measurements of aluminum ion.

Receptor PNI was dissolved in methanol and PNI were diluted with bis-tris buffer to make the final concentration of 10 μM. $Al(NO_3)_3.9H_2O$ was dissolved in bis-tris buffer. A certain amount of the Al^{3+} solution was transferred to each receptor PNI solution. After shaking the vials for a few minutes, UV-vis spectra were taken at room temperature.

Fluorescence measurements of aluminum ion.

Receptor PNI was dissolved in methanol and PNI was diluted in bis-tris buffer to make the final concentration of 10 μM. $Al(NO_3)_3$ was dissolved in bis-tris buffer. The Al^{3+} solution was transferred to each receptor PNI solution prepared above. After shaking the vials for a few minutes, fluorescence spectra were taken at room temperature.

Competition of aluminum ion to other metal ions.

$M(NO_3)_x$ were dissolved in bis-tris buffer, respectively. Each metal solution (10 mM) was added into each PNI solution (10 μM). Then, Al^{3+} solution was added into the mixed solution of PNI containing a competing metal ion.

Job plot measurement of aluminum ion.

$Al(NO_3)_3$ dissolved in bis-tris buffer was added to each PNI solution diluted in bis-tris buffer. Each vial had a total volume of 3 mL. After shaking the vials for a few minutes, fluorescence spectra were taken at room temperature.

UV-vis and fluorescence measurements of cyanide.

Tetraethylammonium cyanide in methanol was transferred to each PNI solution (50 μM). After shaking the vials for a few minutes, UV-vis and fluorescence spectra were taken at room temperature.

Competition with other anions.

Each anion solution (tetraethylammonium salts) was added into 3 mL of each PNI solution (50 μM). Then, CN^- solution was added into the mixture of each competing anion and PNI.

Fluorescent imaging of intracellular Al^{3+} in cells.

Human HeLa cell line were cultured in DMEM (Dulbecco's Modified Eagle Medium) which were supplemented with 100 units/ml penicillin, 100 mg/ml streptomycin, and 10% heat-inactivated fetal bovine serum at 37 ºC in a humidified incubator. Cells were seeded on an 18 × 18 mm cover glass (Marienfeld, Lauda-Koenigshofen, Germany) at density 2×10^5 cells in culture media. HeLa cells were incubated with 1 μM of $Al(NO_3)_3$ in culture media for 4 hour at 37 ºC. After washing with PBS three times to remove the remaining $Al(NO_3)_3$, cells were then incubated with 100 μM PNI for 20 min at RT. The treated cells were washed with PBS and mounted onto a glass slide with ClearMount™ aqueous mounting medium (Invitrogen). The fluorescent images of the mounted HeLa cells were obtained by using a confocal laser scanning microscope (CLSM LSM510, Carl Zeiss) with a 480 nm excitation and LP 520 nm emission filters at various magnifications (200 × to 400 ×).

Acknowledgements

This work was supported by the National Research Foundation of Korea Grant funded by the Korea Government (NRF-2013R1A2A2A03015101, 2012001725, 2012008875), and the

National R&D program of the Ministry of Education, Science and Technology (MEST), Korea: Development of Molecular Sensing Technology (Code number 2012-009832).

Notes and references

Electronic Supplementary information (ESI) available: ESI-MS, Job's plot, and additional NMR.

References

(1) C. S. Cronan, W. J. Walker, P. R. Bloom, *Nature* 1986, **324**, 140-143.

(2) G. D. Fasman, *Coord. Chem. Rev.* 1996, **149**, 125-165.

(3) P. Nayak, *Environ. Res.* 2002, **89**, 101-115.

(4) J. R. Walton, *J. Inorg. Biochem*. 2007, **101**, 1275-1284.

(5) B. Valeur, I. Leray, *Coord. Chem.* Rev. 2000, **205**, 3-40.

(6) J. Barcelo, C. Poschenrieder, *Environ. Exp. Bot.* 2002, **48**, 75-92.

(7) J. Lee, H. Kim, S. Kim, J. Y. Noh, E. J. Song, C. Kim, J. Kim, *Dyes and Pigments* 2013, **96**, 590-594.

(8) S. Kim, J. Y. Noh, K. Y. Kim, J. H. Kim, H. K. Kang, S.-W. Nam, S. H. Kim, S. Park, C. Kim, J. Kim, *Inorg. Chem.* 2012, **51**, 3597-3602.

(9) D. Maity, T. Govindaraju, *Eur. J. Inorg. Chem.* 2011, **36**, 5479-5485.

(10) S. Sen, T. Mukherjee, B. Chattopadhyay, A. Moirangthem, A. Basu, J. Marek, P. Chattopadhyay, *Analyst* 2012, **137**, 3975-3981.

(11) J. Y. Noh, S. Kim, I. H. Hwang, G. Y. Lee, J. Kang, S. H. Kim, J. Min, S. Park, C. Kim, J. Kim, *Dyes and Pigments* 2013, **99**, 1016-1021.

(12) H. M. Park, B. N. Oh, J. H. Kim, W. Qiong, I. H. Hwang, K.-D. Jung, C. Kim, J. Kim, *Tetrahedron Letters* 2011, **52**, 5581-5584.

(13) W. H. Organization, *Guidelines for Drinking-Water Quality*, 1996.

(14) W. Gerhartz, S. Yamamoto, F. T. Campbell, R. Pfefferkorn, J. F. Rounsaville, *Ullmann's Encyclopedia of Industrial Chemistry;* Wiley-VCH: New York, 1999.

(15) S. I. Baskin, T. G. Brewer, *Medical Aspects of Chemical and Biological Warfare;* TMM Publications: Washington, 1997.

(16) H. Hachiya, S. Ito, Y. Fushinuki, T. Masadome, Y. Asano, T. Imato, *Talanta* 1999, **48**, 997-1004.

(17) (a) S.-Y. Chung, S.-W. Nam, J. Lim, S. Park, J. Yoon, *Chem. Commun.* 2009, **20**, 2866-2868. (b) Z. Xu, X. Chen, H. N. Kim, J. Yoon, *Chem. Soc. Rev.* 2010, **39**, 127-137.

(18) K.-S. Lee, H.-J. Kim, G.-H. Kim, I. Shin, J.-I. Hong, *Org. Lett.* 2008, **10**, 49-51.

(19) F. Garcia, J. M. Garcia, B. Garcia-Acosta, R. Martinez-Manez, F. Sanceno, J. Soto, *Chem. Commun.* 2005, **22**, 2790-2792.

(20) J. V. Ros-Lis, M. D. Marcos, R. Martinez-Manez, K. Rurack, J. Soto, *Ange*w. *Chem. Int. Ed.* 2005, **44**, 4405-4407.

(21) C.-L. Chen, Y.-H. Chen, C.-Y. Chen, S.-S. Sun, *Org. Lett.* 2006, **8**, 5053-5056.

(22) M. Jamkratoke, V. Ruangpornvisuti, G. Tumcharen, T. Tuntulani, B. Tomapatanaget, *J. Org. Chem.* 2009, **74**, 3919-3922.

(23) T. Agou, M. Sekine, J. Kobayashi, T. Kawashima, *Chem. Eur. J.* 2009, **15**, 5056-5062.

(24) J. L. Sessler, D.-G. Cho, *Org. Lett.* 2008, **10**, 73-75.

(25) Y. M. Chung, B. Raman, D.-S. Kim, K. H. Ahn, *Chem. Commun.* 2006, 186-188.

(26) R. Badugu, J. R. Lakowicz, C. D. Geddes, *J. Am. Chem. Soc.* 2005, **127**, 3635-3641.

(27) T. W. Hudnall, F. P. Gabba, *J. Am. Chem. Soc.* 2007, **129**, 11978-11986.

(28) P. Anzenbacher Jr., D. S. Tyson, K. Juriskova, F. N. Castellano, *J. Am. Chem. Soc.* 2002, **124**, 6232-6233.

(29) Z. Ekmekci, M. D. Yilmaz, E. U. Akkaya, *Org. Lett.* 2008, **10**, 461-464.

(30) (a) J.H. Lee, A.R. Jeong, I.-S. Shin, H.-J. Kim, J.-I. Hong, *Org. Lett*. 2010, **12**, 764-767. (b) S.-Y. Na, J.-Y. Kim, H.-J. Kim, *Sens. Actuators B: Chem.* 2013, **188**, 1043-1047. (c) K.-H. Hong, H.-J. Kim, *Supramol. Chem.* 2013, **25**, 24-27.

(31) J. Ren, W. Zhu, H. Tian, *Talanta* 2008, **75**, 760-764.

Figure Caption

Figure 1. Emission spectra of PNI (10 μM) in the presence of various metal ions (340 μM) using E_λ = 450 nm in 50 mM Tris buffer (pH = 7.0).

Figure 2. (a) Changes in emission intensity of 10 μM PNI upon the addition of Al^{3+} (0 ~ 0.6 mM), E_λ = 450 nm in 50 mM Tris buffer. (b) Binding isotherm monitored by the fluorescence increase at 515 nm.

Figure 3. Changes in the UV-vis spectrum of PNI (10 μM) as a function of the Al^{3+} concentration in 50 mM Tris buffer.

Figure 4. Aluminum ion (34 μM) response for PNI (10 μM) in the absence and presence of competing metal ions (34 μM) in 50 mM Tris buffer. L stands for PNI.

Figure 5. (a) Changes in the absorption spectrum of PNI (50 μM) in methanol with increasing cyanide concentrations. (b) Color changes on solutions of PNI (50 μM) in the presence of 100 equiv of anions, from left to right: PNI alone, CN^-, F^-, Cl^-, Br^-, I^-, OAc^-, Cl^-, and $H_2PO_4^-$.

Figure 6. Fluoresence spectral changes of 50 μM PNI obtained at 518 nm upon the addition of 100 equiv of various anions in methanol. All fluorescence spectra were acquired with excitation at 450 nm.

Figure 7. (a) Fluoresence titrations of 50 μM PNI with tetraethylammonium cyanide (0 to 500 equiv) in CH_3OH. (b) Ratio of fluorescence intensities at 518 nm as a function of cyanide concentration.

Figure 8. Representative fluorescence images of HeLa cells (a) incubated with PNI only and (b) exposed to 1 μM $Al(NO_3)_3$ with 10 μM PNI. The samples in (b) were incubated with 1 μM $Al(NO_3)_3$ for 4 h and exposed with PNI. Each picture contains DIC images and

fluorescent images (excitation= 480 nm, emission = 520 nm LP). Details are found in Experimental Section. The scale bar represents 20 μm.

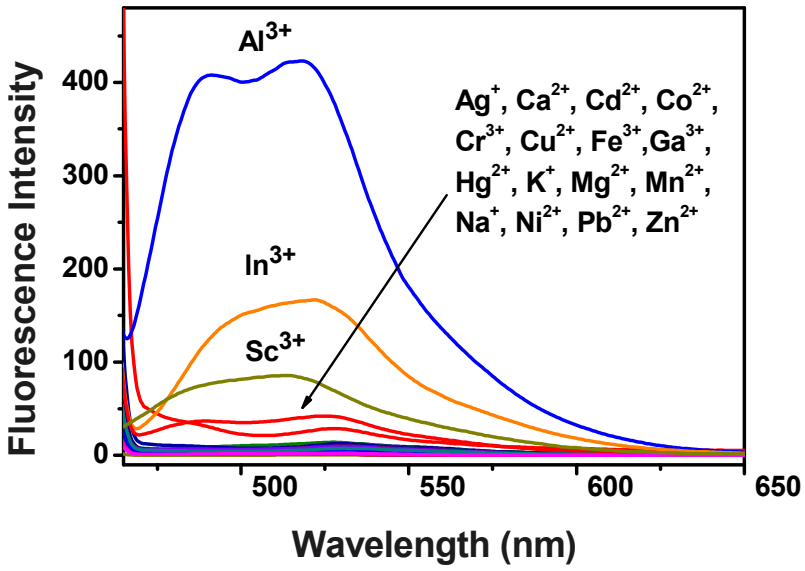

Figure. 1

(a)

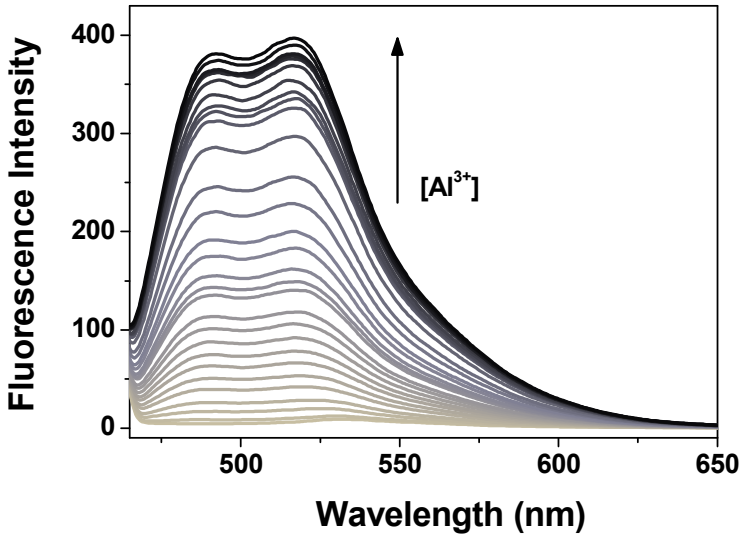

(b)

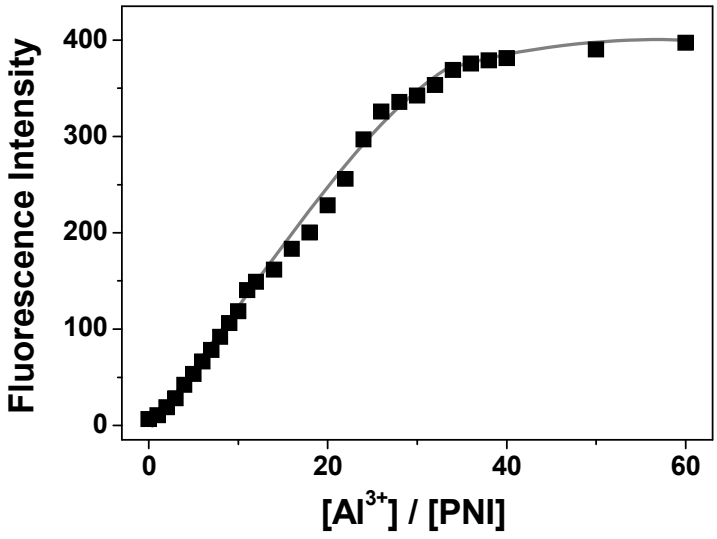

Figure. 2

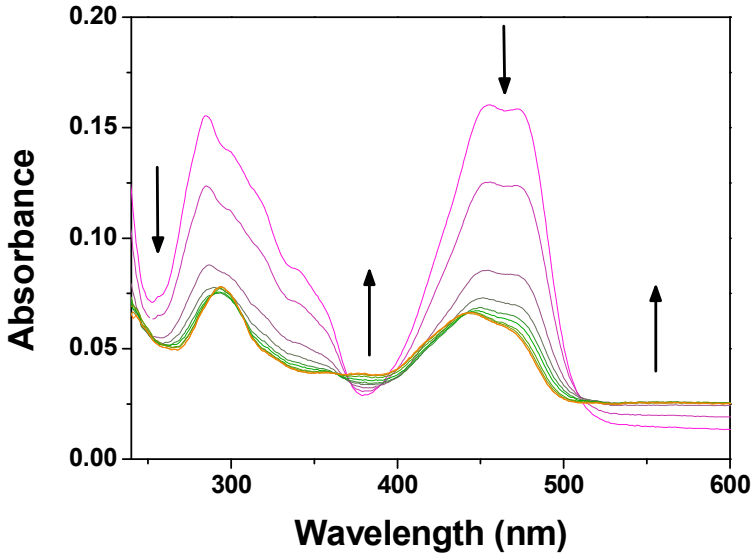

Figure. 3

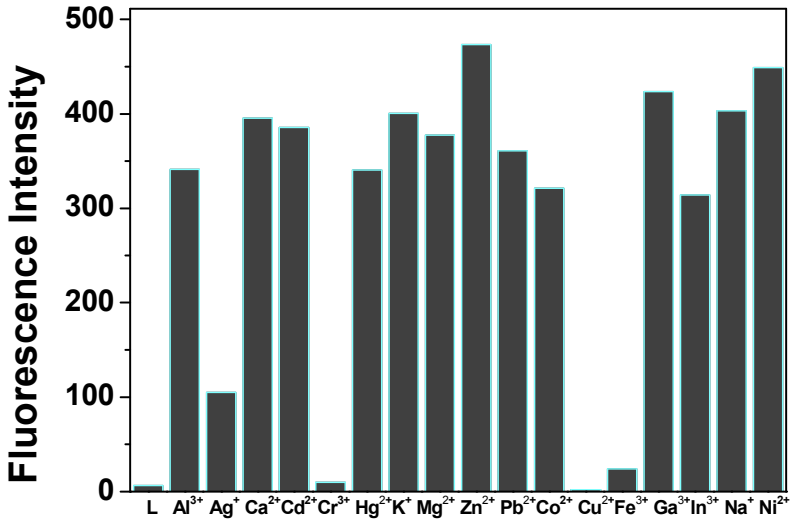

Figure. 4

(a)

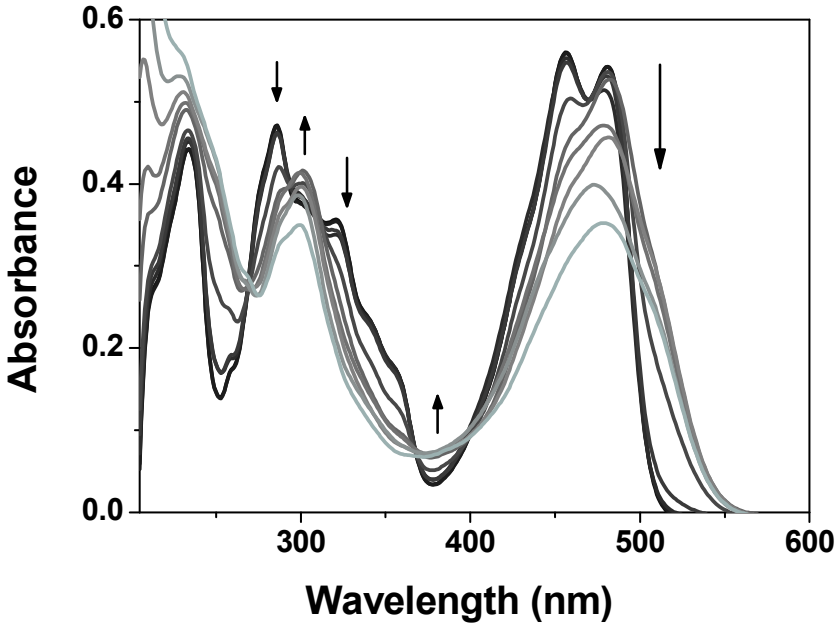

(b)

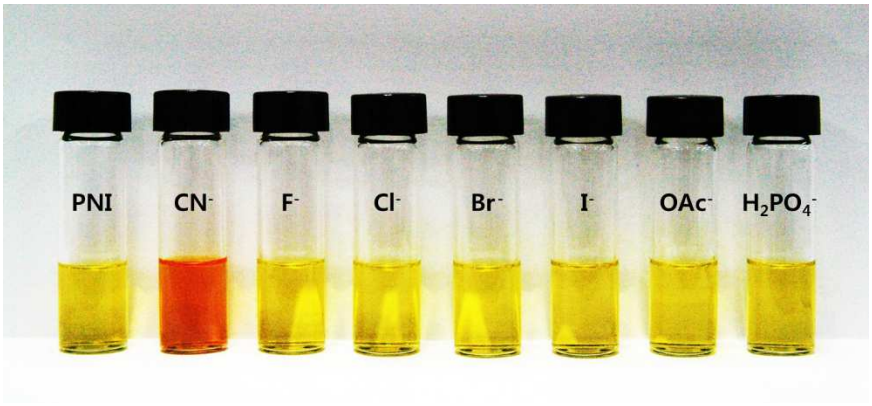

Figure. 5

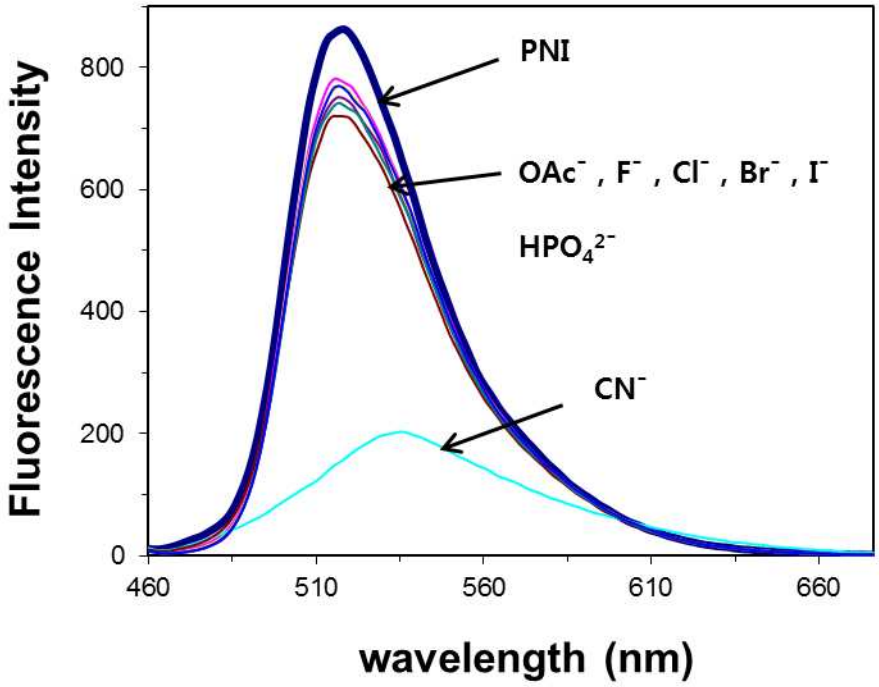

Figure. 6

(a)

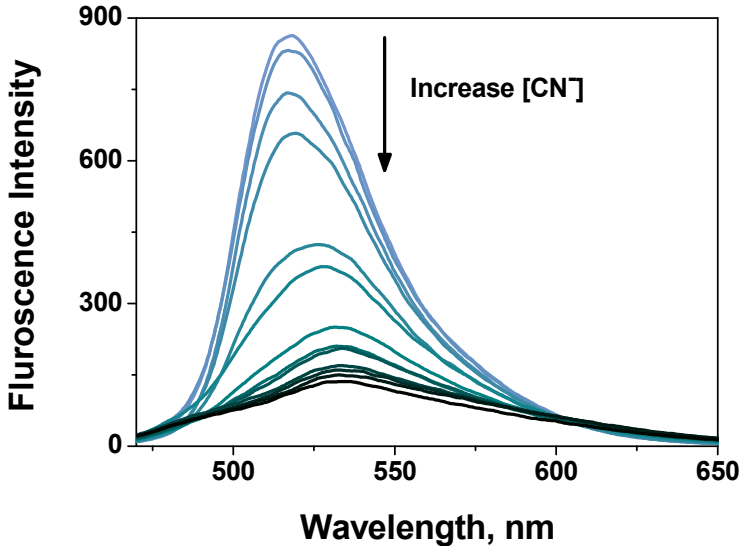

(b)

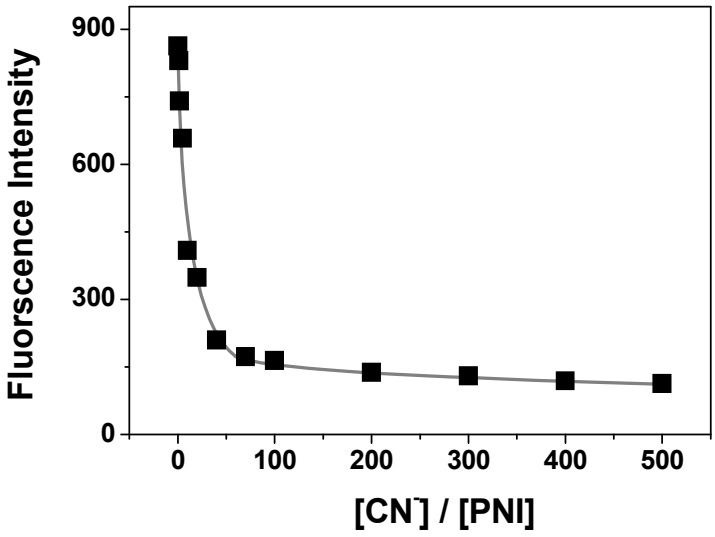

Figure. 7

(a)

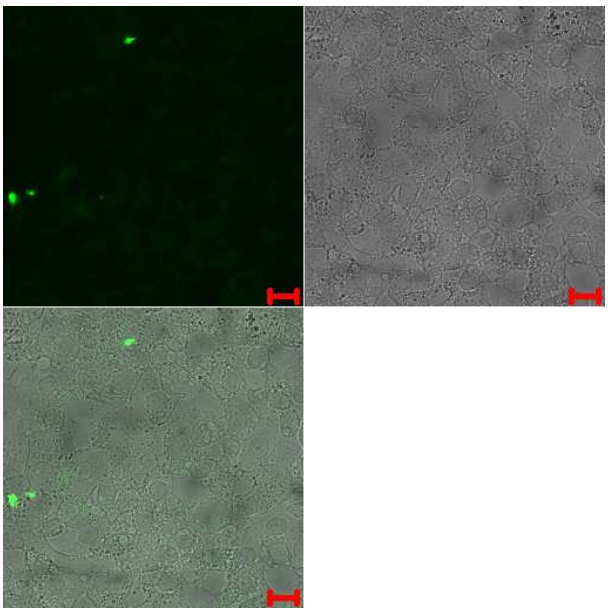

(b)

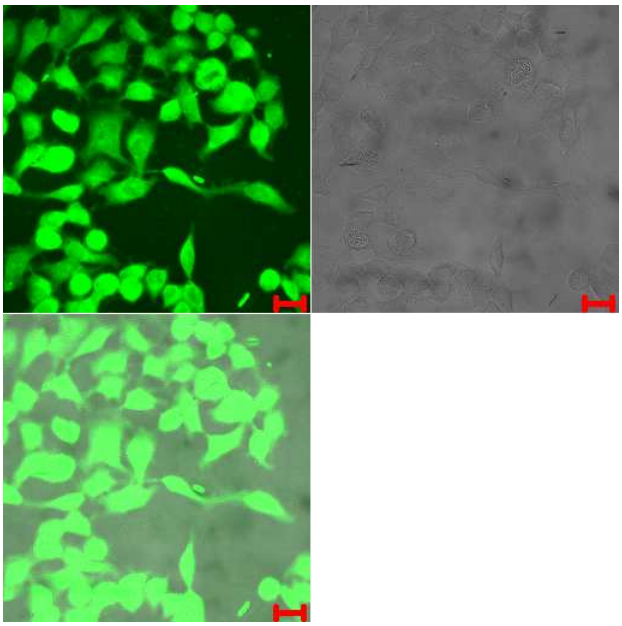

Figure. 8

Graphical abstract